# Considerations For Future Fuels in Naval Vessels

Dr. Rachel Pawling (lead author) CEng MRINA, UCL;
Prof. Richard Bucknall CEng FIMarEST, UCL;
Prof. Alistair Greig CEng FIMarEST, FIMechE PFHEA, UCL

## Synopsis

Emissions regulations aimed at reducing carbon dioxide and other emissions are driving commercial research into alternative fuels. Being government owned, naval vessels are exempt from these regulations, but not auxiliary vessels including the RFA and patrol boats. Some governments have committed to meeting regulations where possible and public or even legal pressure may strengthen a requirement for operation on low-or zero emissions fuels in future, even if only in peacetime. These new fuels present major challenges for naval use, such as lower energy density, increased toxicity, increased flammability and explosion risk, which has implications on storage and use. This paper summarises ongoing work using the ZEOLIT tool, previously presented at INEC 2018, to assess the overall ship impacts of adopting alternative fuels over a range of warship sizes, rather than single exemplar designs. Application of methanol and ammonia to a generic frigate design has been found to lead to increases in size that do not seem excessive, and that more efficient but expensive machinery (fuel cells) is desirable as reductions in displacement are significant compared to increases in cost.

**Keywords**

Fuels, fuel cells, design methods, methanol

## Authors Biographies

Dr. Rachel Pawling is a Lecturer in Ship Design at UCL, teaching the subject of ship design to undergraduate and postgraduate students. She obtained her PhD in computer aided ship design in 2007 subsequently continuing her research in projects funded by the EC, UK and US governments.

Prof. Richard Bucknall is the Professor of Marine Systems Engineering and the Vice Dean (Research) Department of Mechanical Engineering UCL. His research interests include electrical power systems, marine propulsion, and low-carbon technology and he has published over 250 articles in engineering science journals, conferences, and press.

Prof. Alistair Greig is the Professor of Marine Engineering with the Deputy Head (Education) Department of Mechanical Engineering UCL. His research focuses on ship concept design and ways to improve ship efficiency. He has a keen interest in Engineering Education and is a Principal Fellow of the UK Higher Education Academy.

## 1. Introduction

Air emissions regulations at both global and regional / national level are driving research into alternative marine fuels. Being government owned vessels, naval ships would normally be exempt from these regulations, but the ability to operate on such fuels may become a requirement for future combatants due to their availability, or to avoid emissions in domestic and friendly waters. In the near-term availability of new fuels will be an issue, while in the longer-term legacy fuels will become increasingly more difficult and expensive to source and supply. These fuels present challenges for naval use including lower energy density, increased toxicity, increased flammability and explosion risk. Future ship fuelling options have been examined in both wide surveys, e.g. [DNV-GL, 2019], [Krants, Søgaard & Smith, 2022], [DNV, 2022] and specific examples including methanol [Astley, Grasman, & Stroeve, 2020] and Gas-To-Liquid [Tol & Linden, 2018]. LNG has seen some use on Ocean Patrol Vessels, such as the Finnish Turva and Norwegian Berentshav class, having dual-fuel engines capable of using LNG or diesel. Air Independent Propulsion (AIP) submarines are operational using hydrogen (e.g. German Type 212) or alcohols (e.g. the ethanol fuelled MESMA system).

Recent UCL MSc ship designs have been set the requirement to operate on future fuels [Pawling, 2022a], the concept being that cost and availability will drive adoption of these energy sources during peacetime, with reserves of marine diesel oil / NATO F-76 retained for use in wartime where its safety advantages are most valuable. A wider study was required to gain a broader understanding of the impacts on a range of ship designs and provide guidance to the students in the early stages of the design process, where the use of alternative fuels may require different sizing assumptions. The first phase of this study was reported in [Pawling, 2022b] and used the ZEOLIT design tool to examine the impact of alternative fuels on an Ocean Patrol Vessel (OPV).

## 2. The ZEOLIT Design Tool

ZEOLIT (Zonal Exploration Of Layout and Impacts Tool) is a UCL-developed Excel tool for the early-stage design of ships. It has been applied to the investigation of the impact of EM railguns on small combatants, described in [Pawling, Farrier & Bradbeer, 2018] and [Pawling, Farrier & Bucknall, 2018]. Derived from a thought experiment on whether some types of early-stage design studies might be best carried out with a tool that deliberately limited the level of detail, ZEOLIT divides the ship into 32 regions; 8 sections along the length of the ship, and four levels (lower hull, upper hull, lower superstructure and upper superstructure).

A "mask" describes what proportion of each region is available, spaces being allocated to these regions on a profile view, with distributed spaces assigned fractions per region. Rather than iteratively balance the design, ZEOLIT applies the layout to each entry in a database of generic envelopes, retaining those options where the numerical balance (weight and displacement, volume required and available) are within user-specified limits. Table 1 from Pawling, Farrier & Bradbeer, 2018 summarises the approach to defining the ship envelope and layout in ZEOLIT.

Table 1: Layout modelling in ZEOLIT [Pawling, Farrier & Bradbeer, 2018]

**Reference Volume**

| | Stern H | G | F | E | D | C | B | Bow A | 19393 |
|---|---|---|---|---|---|---|---|---|---|
| 2 SS H | 799 | 992 | 1338 | 922 | 1370 | 816 | 749 | 309 | 7295 |
| 1 SS L | 420 | 522 | 704 | 485 | 721 | 430 | 394 | 163 | 3840 |
| -2 No 2 | 446 | 554 | 747 | 515 | 764 | 456 | 418 | 172 | 4072 |
| -3 H L | 123 | 397 | 728 | 712 | 977 | 734 | 432 | 83 | 4186 |
| 19393 | 1788 | 2465 | 3517 | 2635 | 3832 | 2435 | 1994 | 727 | |

Pre-calculated hull option, showing the possible internal volume for the hull and a notional full-height-full-width-full-length single block superstructure.

**Geometry Disposition**

| | Stern H | G | F | E | D | C | B | Bow A | 20 |
|---|---|---|---|---|---|---|---|---|---|
| 2 SS H | 0 | 0 | 0 | 0 | 0.5 | 0 | 0 | 0 | 0.5 |
| 1 SS L | 0 | 0 | 1 | 1 | 1 | 0.5 | 0 | 0 | 3.5 |
| -2 No 2 | 1 | 1 | 1 | 1 | 1 | 1 | 1 | 1 | 8 |
| -3 H L | 1 | 1 | 1 | 1 | 1 | 1 | 1 | 1 | 8 |
| 20 | 2 | 2 | 3 | 3 | 3.5 | 2.5 | 2 | 2 | |
| Number | 21 | | | | | | | | |

"Mask" of the available envelope, which defines how much of the pre-calculated hull is actually used. In this example the hull has a single superstructure block amidships with a small bridge deckhouse (layout zone D-2).

**Item Distribution Inspector**

4

| | Stern H | G | F | E | D | C | B | Bow A | 1 |
|---|---|---|---|---|---|---|---|---|---|
| 2 SS H | 0 | 0 | 0 | 0 | 0 | 0 | 0 | 0 | 0 |
| 1 SS L | 0 | 0 | 0 | 0 | 0 | 0 | 0 | 0 | 0 |
| -2 No 2 | 0 | 0 | 0 | 0 | 0 | 0 | 0 | 0 | 0 |
| -3 H L | 0 | 0.25 | 0.1 | 0 | 0.25 | 0.4 | 0 | 0 | 1 |
| 1 | 0 | 0.25 | 0.1 | 0 | 0.25 | 0.4 | 0 | 0 | |

Inspecting Liquid Fuel Tanks

Number 4

Spaces and equipment are then assigned to layout-zones. Distributed items, such as fuel tanks, can be assigned to multiple zones as fractions. Alternatively, a pseudo-random assignment could be used where the designer specifies the probability of being in a certain layout zone.

**Current Volume**

FG: move

| | Stern H | G | F | E | D | C | B | Bow A | 2406 |
|---|---|---|---|---|---|---|---|---|---|
| 2 SS H | 0 | 0 | 0 | 0 | 187 | 0 | 0 | 0 | 187 |
| 1 SS L | 0 | 0 | 0 | 0 | 0 | 0 | 0 | 0 | 0 |
| -2 No 2 | 0 | 0 | 104 | 27 | 0 | 0 | 0 | 0 | 131 |
| -3 H L | 255 | 187 | 355 | 759 | 258 | 274 | 0 | 0 | 2088 |
| 2406 | 255 | 187 | 459 | 786 | 445 | 274 | 0 | 0 | |

The current volume required in each layout-zone calculated for the entire "move" function (i.e. machinery, fuel tanks etc.)

**Current Total Volume**

Update totals

| | Stern H | G | F | E | D | C | B | Bow A | 9280 |
|---|---|---|---|---|---|---|---|---|---|
| 2 SS H | 0 | 0 | 0 | 0 | 332 | 0 | 0 | 0 | 332 |
| 1 SS L | 0 | 9 | 575 | 447 | 474 | 163 | 9 | 0 | 1676 |
| -2 No 2 | 448 | 496 | 621 | 428 | 647 | 401 | 273 | 443 | 3758 |
| -3 H L | 275 | 435 | 504 | 954 | 381 | 466 | 303 | 196 | 3514 |
| 9280 | 723 | 940 | 1699 | 1830 | 1834 | 1030 | 584 | 639 | |

This aggregation can be repeated over all functions and all layout zones to calculate the total volume (and weight) in each zone.

ZEOLIT returns results as a list of ship size options that meet the specified numerical balance (usually within +/- 5%), with additional data such as the balance of volume per region. These can be aggregated into a single profile as shown in Figure1. In this view, positive values mean more options have excess space in that region than have insufficient space, and negative values mean the opposite. A value of zero means either all options have an acceptable balance of space for that region, or that equal numbers have too much and too little space. For example, Figure 1 shows that the ends of the hull have excess space, whilst the superstructure is largely balanced considering the required and available volumes.

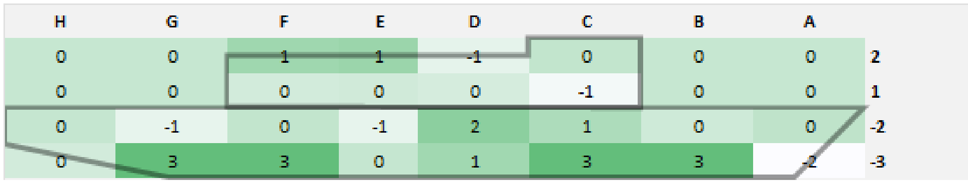

Figure 1: Example profile view for the OPV study with ammonia fuel [Pawling, 2022b].

## 3. Future Marine Fuels

The key characteristics of some of future fuels considered for the maritime sector are summarised in Table 2. Most of these will be familiar to the reader, a possible exception being the Liquid Organic Hydrogen Carrier, or LOHC. These complex hydrocarbons can be reversibly de- and re- hydrogenated [Rude et al., 2022], as opposed to methanol, for which the reactant products are hydrogen, water and $CO_2$. The de-hydrogenated form of the LOHC will generally have similar physical properties and in many cases the chemicals involved are common solvents. The main problems with LOHCs are the small amount of hydrogen carried by weight, and the large amounts of energy (heat) needed to drive the reaction.

Table 2: Characteristics of some alternative fuels of interest [Pawling, 2022b].

| Fuel | Typical density (te/m$^3$) | Typical Lower Heating Value (MJ/kg) | Storage |
|---|---|---|---|
| **F-76 (reference)** | 0.85 | 41 | Atmospheric pressure and temp, arbitrary geometry |
| **Methanol** | 0.79 | 20 | Atmospheric pressure and temp, arbitrary geometry, dry air |
| **Ammonia** | 0.682 | 18.6 | High pressure tank -or- chilled to -33.6deg C, atmospheric pressure |
| **LNG** | 0.45 | 49 | Cryogenic tank |
| **Liquid Hydrogen** | 0.07085 | 120 | Cryogenic tank |
| **GTL** | 0.78 | 44 | Atmospheric pressure and temp, arbitrary geometry |
| **LOHC** | 0.984 | 5.98 * | Atmospheric pressure and temp, arbitrary geometry |

* for benzyltoluene containing 50kg hydrogen per tonne

The first phase of this study examined the application of methanol ($CH_3OH$), Ammonia (NH3) and an LOHC to an OPV. The key results are summarised in Table 3 below where alternative fuels suggest a larger vessel with a higher fuel fraction. The increases in size were not as extreme as had been feared although the design "style" of the vessel would have to change, with the proportionately heavier fuel tanks leading to a ship with excessive volume in the superstructure if current warship arrangements styles are retained.

Table 3 Comparison of results for the OPV study [Pawling, 2022b].

| Variant | Baseline | Methanol ICE | Methanol HT-PEM | Methanol SOFC-GT | Ammonia SOFC-GT | LOHC |
|---|---|---|---|---|---|---|
| **Modal Displacement Range (tonnes)** | 2018 - 2078 | 2193 - 2248 | 2219 - 2264 | 2125 - 2189 | 2400 - 2439 | 2508 - 2518 |
| **Average Fuel Fraction** | 0.110 | 0.204 | 0.188 | 0.180 | 0.173 | 0.267 |
| **Max. delta-T, (m)** | 0.384 | 0.707 | 0.664 | 0.672 | 0.609 | n/a |

A fuel that contains no carbon, such as hydrogen or ammonia, will produce no $CO_2$ emissions in use. However, it may still have environmentally significant emissions. Hydrogen has a global warming potential of 5.8 times $CO_2$ over a 100-year period, potentially released via leaks and unreacted fuel in exhaust streams. Combustion processes using atmospheric air will always produce nitrous oxides (NOx), and nitrogen-rich fuels such as ammonia will increase this.

Commercial users will be restricted by whether regulations permit "net zero", where a carbon-containing fuel such as methanol is acceptable, so long as it is manufactured using atmospheric carbon dioxide. The international trade in biofuels has already proven controversial as it can result in emissions simply being outsourced [Brack, Birdsey & Walker, 2021] and achieving a reliable net-zero accreditation process via IMO may be difficult. This may be simpler to achieve within a national or alliance production system supplying the smaller volumes required by military operators.

## 4. Fuel Cells

Table 4 provides some generic characteristics of prime mover types of interest, including near-term fuel cells of the Proton Exchange Membrane (PEM) and Solid Oxide (SO) types. Whilst fuel cells are currently heavier and larger than internal combustion engines this is likely to improve in time and they are much more efficient, particularly where waste heat can be used in Combined Heat and Power (CHP) arrangements. The "true" fuel for a fuel cell is hydrogen, supplied pure or extracted from a hydrogen carrier (e.g. methanol) by a reformation process, an energy-intensive high-temperature process. High temperature cells are capable of reforming their own fuel and the values in Table 4 include reforming equipment. It should be noted that not all fuel cells can use all hydrogen sources. PEM fuel cells, for example, are particularly vulnerable to contamination with sulphur (from reformed diesel), carbon dioxide, and ammonia.

Table 4: Characteristics of some prime mover types of interest

| Type | te/MW | $m^3$/MW | Relative Cost | % Efficiency | Duty Cycle | Notes |
|---|---|---|---|---|---|---|
| **High speed diesel mechanical** | 3.53 | 3.69 | 0.77 | 44 (m) | Heavy | Engine only |
| **Medium speed diesel mechanical** | 4.56 | 28.56 | 1 | 46 (m) | Heavy | Engine only |
| **Gas turbine mechanical** | 0.84 | 4.08 | 1.78 | 40 (m) | Heavy | Module only |
| **HT-PEM, automotive** | 18.70 | 9.23 | 0.2 | 50 (e) | Light | Complete system [Jensen, 2019] |
| **Generic automotive SOFC** | 1.00 | 1.00 | | 60 (e) | Light | Stack only [Bossel, 2005] |
| **SOFC (Domestic, CHP)** | 125.00 | 437.00 | 1.76 | 52 (e) 90 (CHP) | Medium | Complete system [Kyocera, 2017] |
| **SOFC-GT hybrid (aircraft)** | 3.43 | 3.96 | | 70.4 (e) | Heavy | Complete system [Whyatt & Chick, 2012] |
| **SOFC-GT hybrid (Industrial, CHP)** | 145.24 | 619.96 | 1.50 | 55 (e) 73 (CHP) | Heavy | Complete system [Mitsubishi Power, 2021] |
| | **te/kVA** | **$m^3$/kVA** | | | | |
| **High speed diesel generator** | 8.08 | 7.52 | 1.06 | 44 (e) | Heavy | Engine and alternator |

Fuel cell technology is being driven by other industries; land, automotive or aerospace, and detailed comparisons of technologies can be found in the literature e.g. [Advanced Propulsion Centre UK, 2020]. Automotive fuel cells have seen a significant drop in costs over the last decade, with low temperature PEMS being cheaper, on a system per-kW basis, than internal combustion engines. However, these are light-duty devices and these savings have not yet extended to the heavy duty types required for marine use, with a relative cost of three times a medium speed diesel engine assumed here.

The use of aerospace derivative fuel cells is of interest as unlike automotive systems, they are designed for a high duty cycle, with the demand changing comparatively little through flight [Whyatt & Chick, 2012]. Hybrid SOFC-GT arrangements, where a gas turbine is driven from the hot exhaust of the fuel cell, are capable of very high efficiencies, near 60% with simple cycle gas turbines and up to 70% if complex cycle machines are used. An alternative arrangement to achieve very high overall efficiency is to use waste heat for domestic or process heating, in a Combined Heat and Power (CHP) arrangement. Whilst a combined SOFC-GT-CHP arrangement has been examined for use aboard ship [Duong et al. 2022], this level of complexity is seen as being ill-suited to warships due to the weight and space limitations, and significant time at part load.

The space demands of fuel cells requires consideration. Automotive and aviation examples will generally be designed for minimum size and maintenance by removal from the vehicle. Whilst repair-by-replacement may be practical on a ship, space will still be required to access modules. Figure 2 illustrates the difference in arrangements between an automotive HT-PEM, aviation SOFC-GT hybrid, and naval fuel cell. Additionally, it must be remembered that fuel cells have a similar demand for air (and thus ducting) as a diesel engine, albeit without the need for silencers.

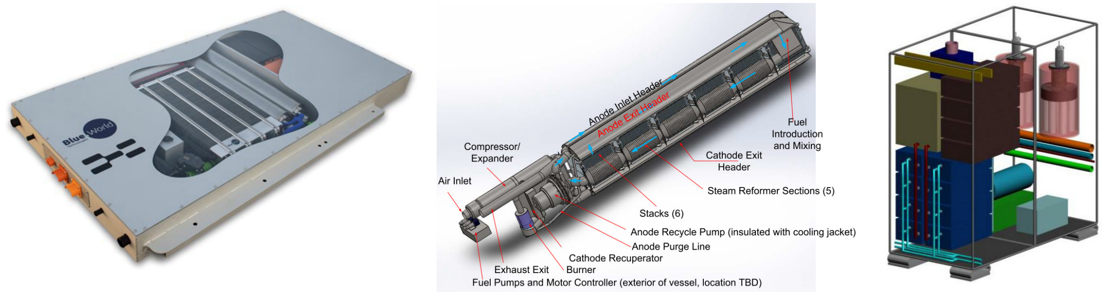


Automotive Aviation Marine

Figure 2: A comparison of automotive [Jensen, 2019], aviation [Whyatt & Chick, 2012] and marine [Kuseian & Hoffman, 2002] fuel cells showing differences in arrangement

Another aspect of fuel cell technology that may prove significant is the possibility for multi-fuelling [Sasaki et al., 2004]. This has been demonstrated in the lab, with high-temperature SOFC being the main fuel cell type of interest. These would allow a range of fuels such as hydrogen, ammonia, methane or methanol to be used in a single cell, albeit with some changes in performance.

A feature of fuel cells is that they are most efficient at part loads. Figure 3 illustrates the generic efficiency curves used in the study. These were non-dimensionalised and applied to the reference SFC (assumed to be at the most efficient point) for each machinery selection to determine the part-load fuel consumption. In practice low loadings for the diesels and gas turbines would be avoided.

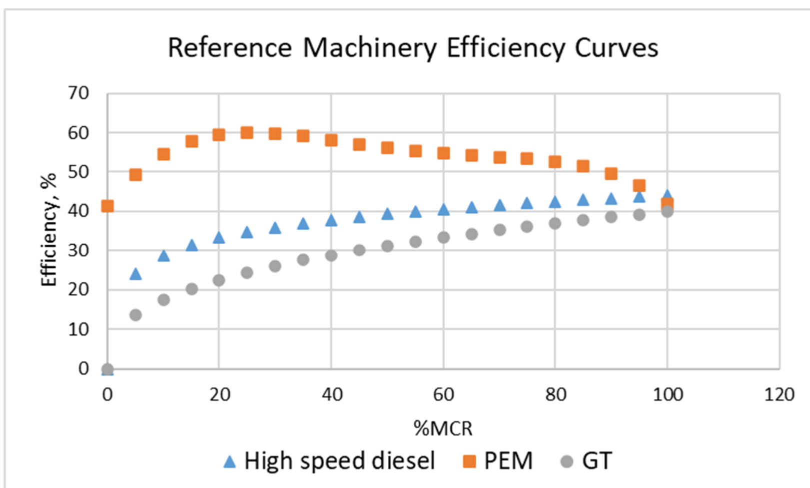


Figure 3: Generic efficiency curves for the three main types of prime movers, based on data from Sandia [Pratt & Chan, 2017], MTU and Rolls Royce data sheets

This raises the question of whether over-sizing fuel cells would be worthwhile, to reduce fuel consumption. A brief, simplified investigation into this aspect was carried out, with the design point for the fuel cells being varied between 30 and 70%. All fuel cell and a combined fuel-cell cruise with gas turbine boost were investigated with the combined mass and volume of the prime movers and fuel recorded for each option. The fuel cell was a high-temperature PEM device, with methanol fuel. The results are shown in Table 5 below.

The fuel savings from the improved efficiency of designing the fuel cells for a lower % loading are greatly offset by the increase in fuel cell size and weight. Unless fuel costs are very high, or there are other technical concerns, such as achieving a lower average duty cycle, fuel cells will probably be designed for relatively high loadings.

Fuel cells generally have a slower response to changes in load compared to diesels and gas turbines, requiring additional short term energy storage local to the fuel cells. Fuel cells are used in combination with batteries and capacitors in many applications. Whilst significant from a system design perspective, the actual stored energy required appears to be low; the Sandia work [Pratt & Chan, 2017] including supercapcitors equivalent to 3.6 seconds of full power, and batteries equivalent to 23 seconds full power. For the fuel cell design variants these were rounded up to 4 and 30 seconds respectively. This led to ESS masses in the order of hundreds of kilogrammes total, rather than the tonnes for the backup battery.

Table 5: impact of fuel cell design point on weight and space demands

**All fuel cell topology**

| Design Point, % | 30 | 40 | 50 | 60 | 70 |
|---|---|---|---|---|---|
| **Fuel, te** | 635 | 653 | 675 | 693 | 704 |
| **Prime mover mass, te** | 1326 | 995 | 800 | 670 | 579 |
| **Prime mover volume, m3** | 2142 | 1607 | 1292 | 1082 | 935 |
| **Prime mover and fuel mass, te** | 1961 | 1647 | 1474 | 1362 | 1282 |
| **Prime mover and fuel volume, m3** | 3116 | 2608 | 2327 | 2144 | 2013 |

**Fuel cell + GT boost topology**

| Design Point, % | 30 | 40 | 50 | 60 | 70 |
|---|---|---|---|---|---|
| **Fuel, te** | 719 | 732 | 748 | 761 | 769 |
| **Prime mover mass, te** | 477 | 367 | 295 | 256 | 224 |
| **Prime mover volume, m3** | 858 | 680 | 564 | 501 | 449 |
| **Prime mover and fuel mass, te** | 1196 | 1098 | 1043 | 1017 | 992 |
| **Prime mover and fuel volume, m3** | 1938 | 1781 | 1691 | 1650 | 1609 |

## 5. Power and Propulsion System Topologies and Sizing

Three main machinery topologies were investigated in this study: Combined Diesel-electric And Diesel (CODLAD), Combined Diesel-Electric and Gas turbine (CODLAG), and Combined Fuel Cell And Gas turbine (COFCAG). In all cases, cruise propulsion was provided via geared electric motors, with the boost machinery driving the shafts through gearboxes.

ZEOLIT selects combinations of prime movers based on the power demand for any given design option. The permitted combinations are given in a list, with one unique entry for each 250kW increment (for generators) or 1MW increment (for mechanical propulsion). The use of a pre-populated list means that, for some power requirements a single GT might be used, whilst for others a pair. Similarly for diesel boost arrangements either one or two engines were used per shaft.

Generators were sized based on two cruise speeds; a slow cruise of 7 knots and a fast cruise (14 knots for the CODLAD baseline, 21 knots for variants with GT boost, to avoid under-loading the GTs), with hotel loads based on the combat system, complement, internal volume etc. Two pairs of DGs (or two groups of fuel cells) being sized; one large and one small. Fuel cells were assumed to be assembled from 500kWe units, based on US Navy studies [Kuseian & Hoffman, 2002]. Generic curves of the relationship between SFC and percentage loading were used to calculate the SFC for each operating point, based on a reference value for the machinery.

## 6. The Frigate Design Study

The main capabilities and combat systems are listed in Table 6 and illustrated in Figure 4. Figure 5 illustrates the distribution of each of the main Functional Groups; FLOAT (which includes void spaces), MOVE, FIGHT and INFRASTRUCTURE. The arrangement was conventional, with propulsion machinery spaces amidships in the lower hull, auxiliary machinery spaces fore and aft; accommodation on No 2 deck and in the forward superstructure, and much of the superstructure taken up by combat systems, boat bays etc.

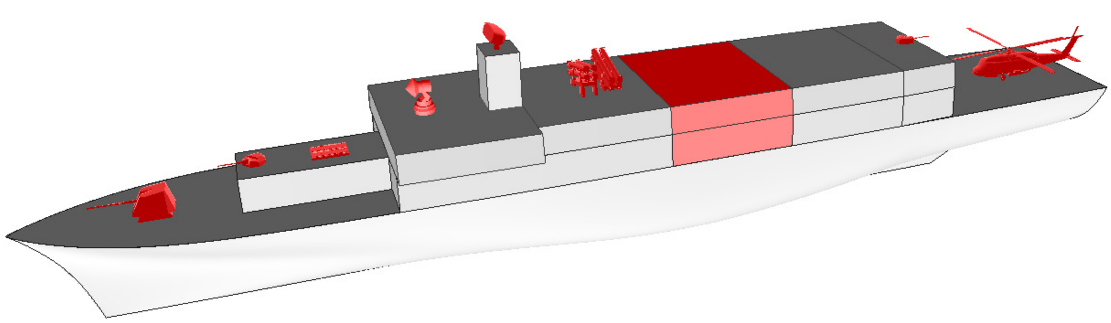

Figure 4: Paramarine visualisation of the baseline design showing main combat systems in red

Table 6: Capabilities and combat systems for the frigate study

| Performance | | Mission Systems | |
|---|---|---|---|
| **Cruise Speed** | 14 knots | **Weapons** | 1 x 76mm gun<br>2 x 30mm guns<br>32 x CAMM SAM<br>8 x Exocet SSM<br>2 x triple torpedo tubes |
| **Maximum Speed** | 28 knots | **Aviation** | 1 x 10te helicopter with hangar<br>1 x 1.5te UAV with hangar |
| **Stores Endurance** | 30 days | **Daughter Craft** | 2 x 7m RIBs<br>2 x 11m RIBs<br>6 x TEU sized modules |
| **Accommodation** | 112 crew, 41 embarked (typical) | **Sensors** | 1 x 3D surveillance radar<br>2 x nav radars<br>1 x electro optical<br>1 x fire control radar<br>1 x hull mounted sonar |

| float | Stern H | G | F | E | D | C | B | Bow A |
|---|---|---|---|---|---|---|---|---|
| SS H | 0 | 0 | 16 | 18 | 252 | 0 | 0 | 0 |
| SS L | 0 | 22 | 38 | 46 | 275 | 9 | 0 | 0 |
| No 2 | 123 | 46 | 5 | 0 | 20 | 8 | 45 | 39 |
| H L | 92 | 127 | 151 | 51 | 102 | 222 | 286 | 247 |

FLOAT

| move | Stern H | G | F | E | D | C | B | Bow A |
|---|---|---|---|---|---|---|---|---|
| SS H | 0 | 0 | 22 | 96 | 96 | 283 | 0 | 0 |
| SS L | 0 | 0 | 11 | 11 | 11 | 11 | 0 | 0 |
| No 2 | 0 | 0 | 18 | 73 | 55 | 13 | 0 | 0 |
| H L | 131 | 88 | 268 | 988 | 1445 | 316 | 163 | 0 |

MOVE

| fight | Stern H | G | F | E | D | C | B | Bow A |
|---|---|---|---|---|---|---|---|---|
| SS H | 0 | 115 | 378 | 375 | 85 | 165 | 0 | 0 |
| SS L | 0 | 134 | 389 | 356 | 106 | 124 | 71 | 0 |
| No 2 | 316 | 0 | 0 | 0 | 0 | 0 | 0 | 69 |
| H L | 0 | 73 | 28 | 0 | 0 | 0 | 47 | 39 |

FIGHT

| infra | Stern H | G | F | E | D | C | B | Bow A |
|---|---|---|---|---|---|---|---|---|
| SS H | 0 | 9 | 16 | 10 | 50 | 5 | 0 | 0 |
| SS L | 0 | 6 | 89 | 19 | 88 | 137 | 12 | 0 |
| No 2 | 4 | 243 | 196 | 170 | 309 | 160 | 110 | 4 |
| H L | 0 | 162 | 313 | 335 | 3 | 255 | 11 | 0 |

INFRASTRUCTURE

Figure 5: Distribution of volume for each of the four functional groups in the baseline design

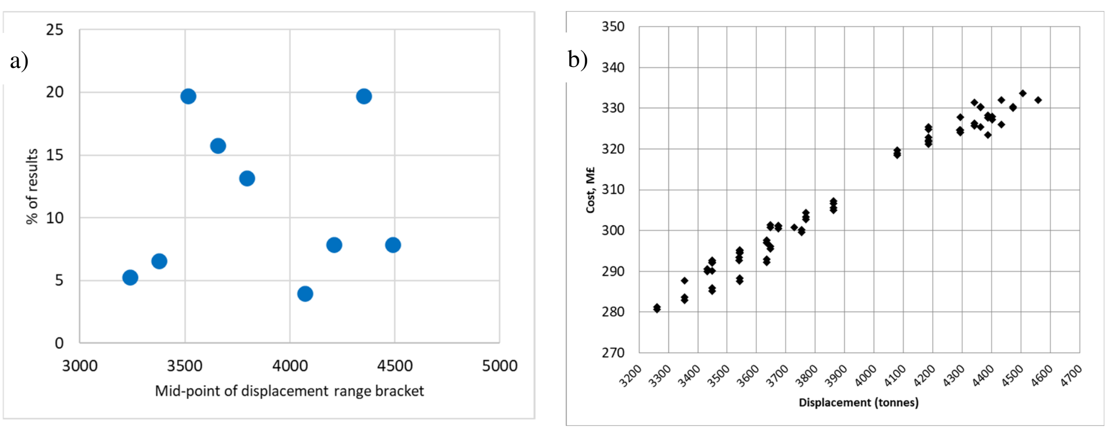


Figure 6: Displacement (a) and cost ranges (b) for the baseline options

The resulting designs were in two clusters, around 3600 and 4400 tonnes, as illustrated in Figure 6 with costs between 290 and 340 million pounds. The presence of clusters in ZEOLIT runs is not unusual, as the machinery data is derived from real-world information so is not uniform over all power ranges, instead featuring steps in power and associated space and weight. A typical machinery fit for one option is shown in Table 7.

The baseline design uses a CODLAD arrangement, with diesel generators supplying hotel loads and propulsion up to a cruise speed of 14 knots and geared diesels providing propulsion above that speed. Diesel engine and generator data was taken from publicly available MTU and Bergen datasheets. The fuel demand was calculated based on the operational profile shown in Figure 7, with the changes in Specific Fuel Consumption (SFC) for different loading accounted for. This generally equated to a range of 9-10,000nm at 14 knots in endurance mode.

Table 7: Typical baseline CODLAD machinery fit

| | |
|---|---|
| **Displacement** | 4467 tonnes |
| **Action stations hotel load** | 1.55MW |
| **Propulsion motors** | 2 x 1.0MW |
| **Diesel generators** | 2 x 0.91MW and 2 x 1.807MW |
| **Boost engines** | 4 x MTU 20V8000 @ 8.2MW each |
| **Fuel capacity** | 456 tonnes F76 |
| **Fuel fraction** | 0.102 |

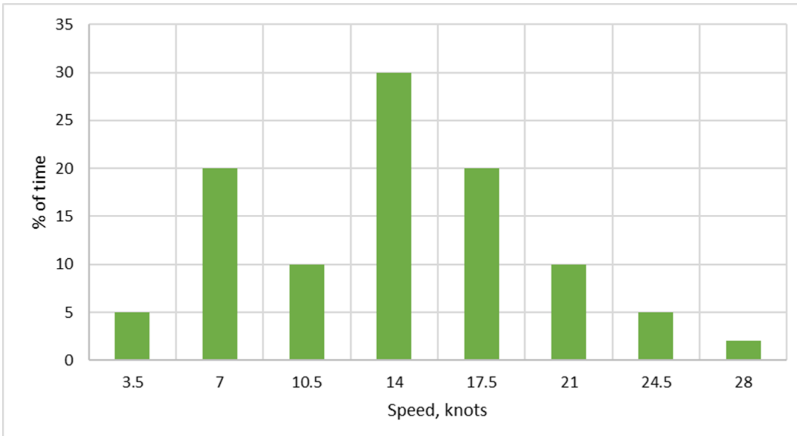

Figure 7: the operating profile used for the frigate study

The baseline frigate design includes a backup battery sized to supply the harbour loads for three hours, at a design Depth of Discharge (DoD) of 40% to prolong life. The batteries were based on Corvus Blue Whale data [Corvus Blue Whale, 2022] and due to the ratio of peak to harbour loads, were generally capable of supplying full combat hotel load for 25 minutes.

A variant of the baseline was produced using CODLAG propulsion, with the boost diesels exchanged for boost gas turbines. This led to a relatively small difference in displacement and cost, as illustrated in Table 8 below. CODLAG options were typically slightly heavier and more expensive than CODLAD, but the former was primarily due to the selection of the speed at which the vessel switched from diesel electric to gas turbine mode, as for some GT options this would lead to operations at a low load, with a very high SFC.

Table 8: Comparison of the baseline designs

| Variant | Baseline CODLAD | Baseline CODLAD 14 knots | Baseline CODLAD 17.5 knots |
|---|---|---|---|
| **Min displacement, te** | 3168 | 3262 | 2887 |
| **Max displacement, te** | 4559 | 4506 | 4362 |
| **Modal displacement, te** | 3516 and 4350 | 3822 | 3256 |

## 7. Methanol Fuel Variants

### *7.1 CODLAD*

As on the previous OPV study, meOH fuel was first investigated whilst retaining the baseline CODLAD machinery topology. The only change to the arrangement was to redistribute the fuel tankage to account for the increased volume. Figure 8 shows the initial results set; red squares represent the ratio of displacement to mass and blue diamonds the ratio of available to required volume. It can be seen that the set of results is very sparse, and all have excess volume (Va/Vr >1). This was due to the increased mass and volume of fuel (in the lower hull) increasing displacement, which led to hullforms with far more volume in the upper hull and superstructure. For this initial run ZEOLIT only selected options with the highest draught to depth ratio (0.5), reinforcing the finding that meOH would generally lead to ships with lower freeboard and smaller superstructures than current designs (for equal displacement).

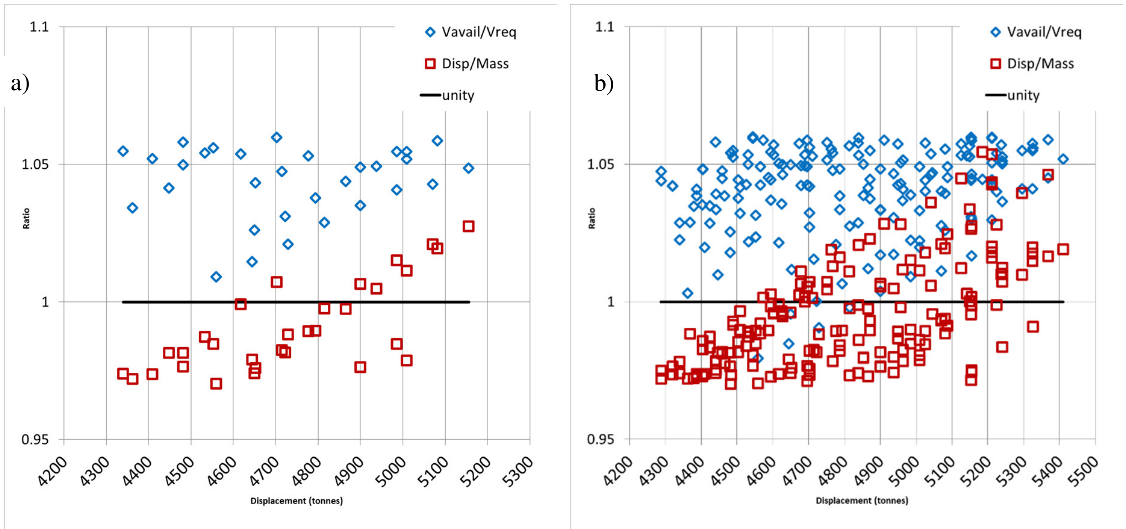

Figure 8: Comparison of results sets for 6% (a) and 9% (b) void volume

The frigate superstructure contains combat system spaces that cannot easily be moved. Reducing freeboard is possible but reduces survivability through loss in reserve of buoyancy. The solution adopted was to increase the void volume fraction from 6% in the baseline to 9% - accepting that the uppermost spaces would be more roomy. As shown in Figure 8 this increased volume requirement led to an increased number of acceptable design options.

Figure 9 shows the overall increase in displacement for the methanol fuelled CODLAD options, with some options being up to a thousand tonnes greater displacement. Fuel fraction doubled and cost was increased by approximately M£10. Using Figures 8 and 9 together a typical size of 4900 tonnes is selected, as this is values for both disp/mass and Va/Vr are around unity in this range.

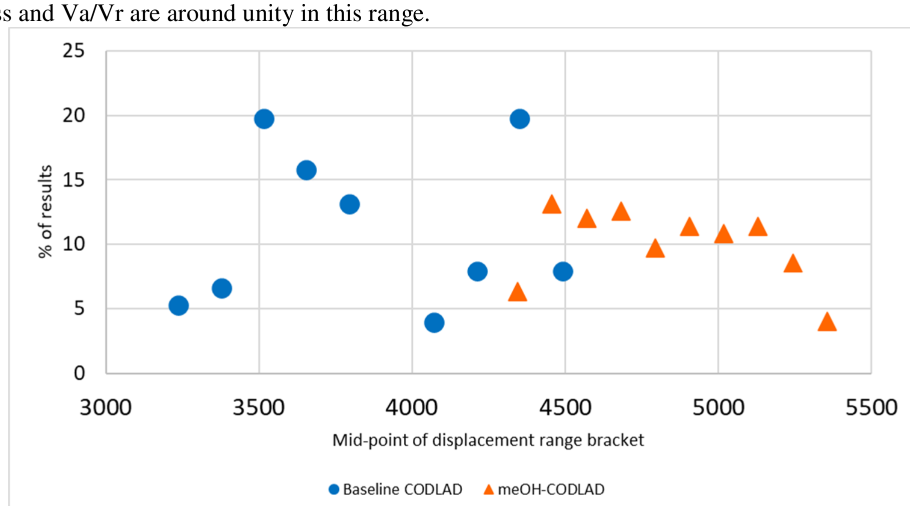

Figure 9: Distribution of displacements for methanol fuel and CODLAD propulsion compared with the F-76 fuelled baseline

### *7.2 Fuel Cells*

A HT-PEM fuel cell was selected, powering high speed electric drive (high speed motors with gearboxes), with GT providing boost power via reduction gearboxes. Void volume allowance was reset to the baseline of 6%, leading to the results shown in Figure 10. Overall, the fuel cell designs are slightly smaller than the meOH-ICE option and does not require additional void volume to achieve design balance within the constraints of modern frigate and destroyer hull style. This latter point is due to the large volume requirement of the fuel cell used in this study. For the same displacement, cost increases by M£10-15, due to the increased cost of the machinery.

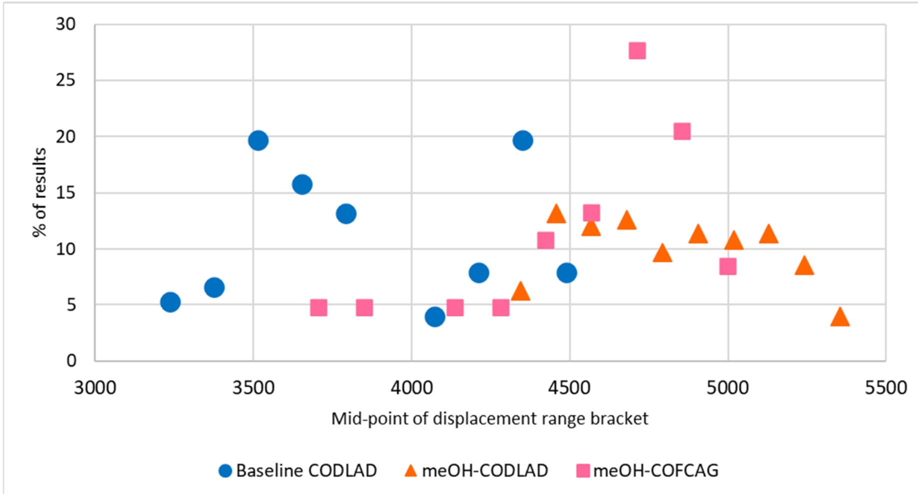


Figure 10: Comparison of meOH and baseline F-76 fuelled options

The initial fuel cell arrangement simply retained that of the diesel machinery, with the fuel cells concentrated in large blocks - this led to some regions in the lower hull being very cramped. As the fuel cells are assumed to be composed of 500kW modules, a distributed generation concept was investigated. Figure 11 compares the aggregated volume availability for the centralised and distributed fuel cell arrangements. Note that lower numbers mean more options are cramped in that region of the design.

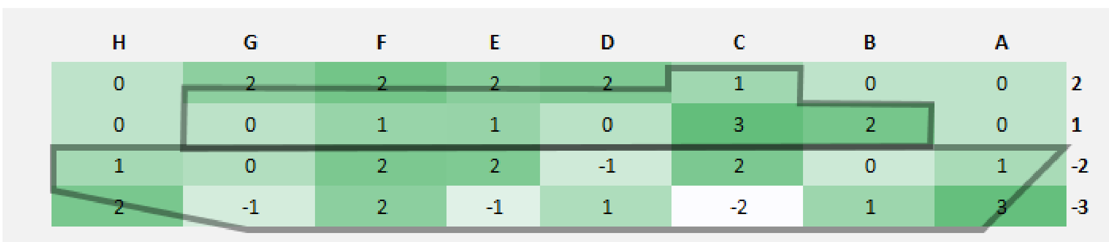


meOH + COFCAG (centralised)

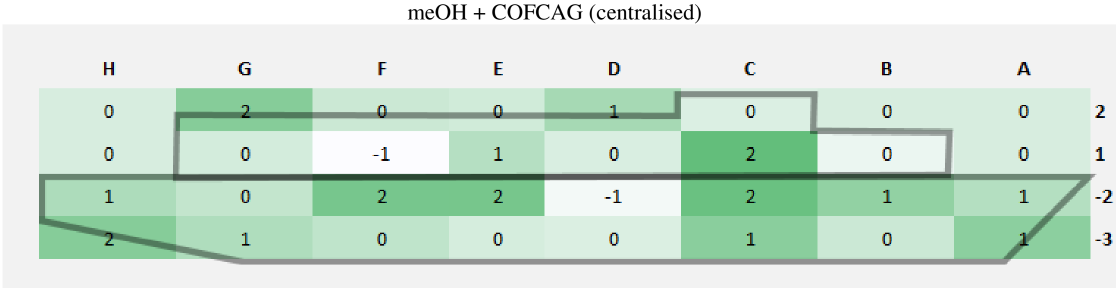


meOH + COFCAG (distributed)

Figure 11: Comparison of volume availability in the centralised and distributed designs

The air supply and exhaust ducting was distributed proportional to the fuel cells, and this leads to the reductions in available volume in the superstructure indicated by lower numbers in Figure 11. The methanol fuel tanks were also distributed along the length of the ship, and the fuel cell and tank distributions are shown in Figure 12. It was found that the need for some large propulsion systems, such as the electric motors and gearboxes, to be aft of amidships led to a design where most fuel cells were located forward.

| | Stern H | G | F | E | D | C | B | Bow A |
|---|---|---|---|---|---|---|---|---|
| SS H | 0 | 0 | 0 | 0 | 0 | 0 | 0 | 0 |
| SS L | 0 | 0 | 0 | 0 | 0 | 0 | 0 | 0 |
| No 2 | 0 | 0 | 0 | 0 | 0 | 0 | 0 | 0 |
| H L | 0 | 0 | 0.15 | 0 | 0.11 | 0.24 | 0.19 | 0 |

Fuel cell machinery distribution. GTs are in region D and motors are in E and F

| | Stern H | G | F | E | D | C | B | Bow A |
|---|---|---|---|---|---|---|---|---|
| SS H | 0 | 0 | 0 | 0 | 0 | 0 | 0 | 0 |
| SS L | 0 | 0 | 0 | 0 | 0 | 0 | 0 | 0 |
| No 2 | 0 | 0 | 0 | 0 | 0 | 0 | 0 | 0 |
| H L | 0 | 0.10 | 0.20 | 0.10 | 0.20 | 0.20 | 0.20 | 0 |

Fuel tank distribution

Figure 12: Proportional distributions of fuel cells (top) and meOH tanks (bottom) in the "distributed" variant.

## 8. Ammonia Fuel

Ammonia is a potential fuel for SOFC and combustion engines, although its use in gas turbines has only recently been demonstrated [Shintaro et al., 2020] and is less developed than methanol fuelling and so a COFCAG ammonia-fuelled arrangement may need to be dual-fuel, with the boost gas turbines fuelled from a hydrocarbon such as methanol. For ammonia, the fuel cells were changed from HT-PEM to SOFC, with the latter based on aerospace technology but with a margin applied to volume to allow for on-board maintenance. Fuel cell cost was held constant per kWe for both types. The resulting design options were similar in size to the methanol – fuel cell variants, as shown in Figure 13.

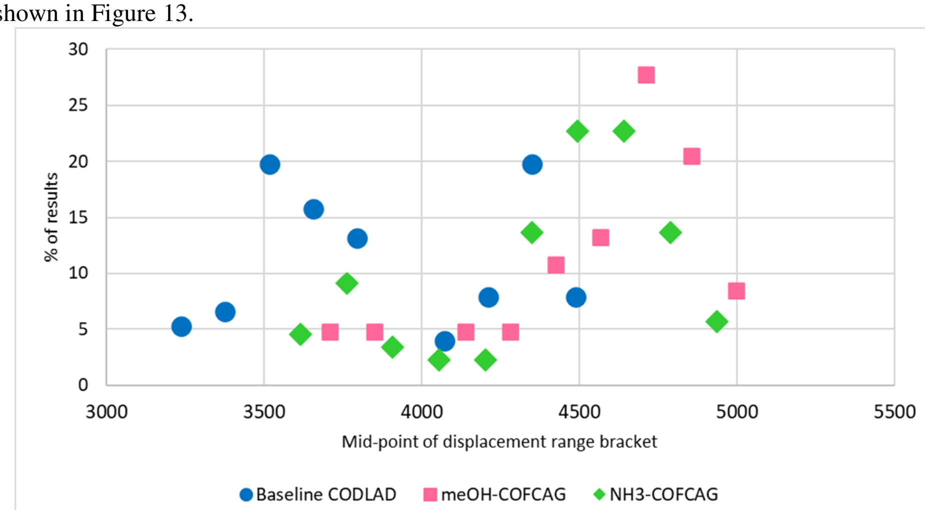


Figure 13: Comparison of options for the baseline, meOH fuel cell and ammonia fuel cell variants

This particular design illustrates an issue with gas turbines that was noted in the previous ZEOLIT studies on railgun-armed vessels; the limited range of sizes led to designs being divided between those with small GTs, and excessive volume in way of the GT space (region D-3), and those with large GTs and too little volume. This is shown in Figure 14 as the "-1" values in region D-3 (due to the GTs) and D1 (due to the GT ducting).

| H | G | F | E | D | C | B | A | |
|---|---|---|---|---|---|---|---|---|
| 0 | 3 | 1 | 0 | 0 | 1 | 0 | 0 | 2 |
| 0 | 0 | 0 | 0 | -1 | 2 | 1 | 0 | 1 |
| 1 | 1 | 1 | 1 | 0 | 0 | 0 | 1 | -2 |
| 2 | 1 | 1 | 1 | -1 | 0 | 3 | 3 | -3 |

Figure 14: Aggregate volume availability across all regions for the NH3-COFCAG variants

The fuel tanks for the baseline design are sized using an operational profile, rather than a range at endurance speed. For a dual fuel option this is particularly significant. Figure 15 illustrates the tonnes of fuel associated with each step in the speed-time operational curve.

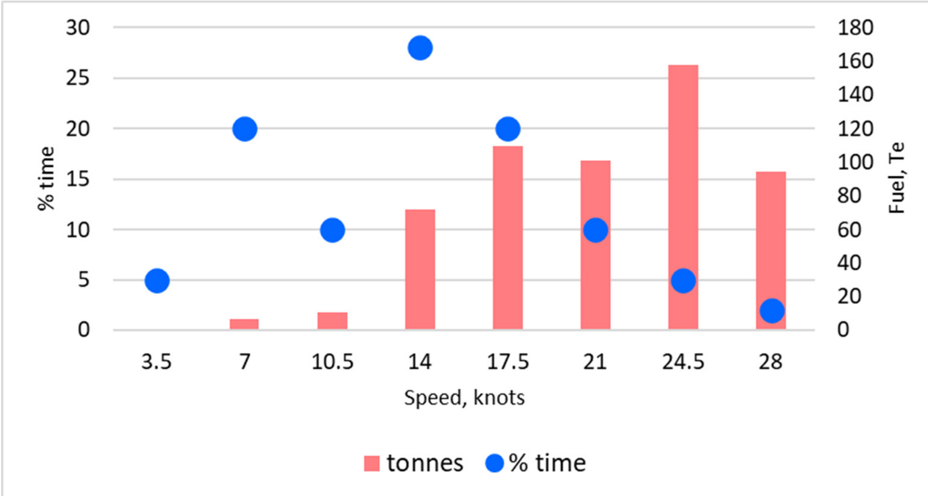


Figure 15: Contribution of each operational point on the total fuel storage

At the high-speed points above 21 knots, using a gas turbine mechanical propulsion and $CH_3OH$ fuel contribute significantly to the overall fuel requirement. A consequence of this is that, with multifuel SOFC, the range achieved running them on methanol fuel only would be a militarily useful 5000-6000nm at 14 knots.

## 9. Conclusions

This paper has presented the second stage of an ongoing project using the UCL developed ZEOLIT early stage design tool to investigate future fuel options for warships. Previous work examined an OPV of approximately 2000 tonnes, and the latest work has focussed on a frigate of 4000 tonnes. Table 9 below summarises some high-level comparisons between the options.

Table 9: Summary of high-level metrics for comparison

| | Absolute Values | | | Relative to Baseline | | |
|---|---|---|---|---|---|---|
| | **Disp, te** | **Cost, M£** | **Fuel Fraction** | **Disp, te** | **Cost, M£** | **Fuel Fraction** |
| **Baseline CODLAD** | 3862 | 307 | 0.104 | 1.00 | 1.00 | 1.00 |
| **Baseline CODLAG** | 3895 | 315 | 0.152 | 1.01 | 1.03 | 1.46 |
| **meOH-CODLAD** | 4817 | 329 | 0.248 | 1.25 | 1.07 | 2.38 |
| **meOH-COFCAG (HTPEM)** | 4565 | 333 | 0.247 | 1.18 | 1.09 | 2.38 |
| **NH3-COFCAG (SOFC)** | 4425 | 330 | 0.184 | 1.15 | 1.08 | 1.77 |

Whilst the OPV study examined some innovative fuels such as LOHC, for the frigate methanol and ammonia have been investigated as these are of interest to the commercial world and thus are likely to be widely available. The values in Table [conclusions] indicate that, despite their lower energy density, these fuels do not drive the frigate design to impractically large sizes. Using fuel cells caused an increase in vessel cost, but a disproportionately greater reduction in size due to increased fuel efficiency (this reduction in size also offsetting some of the prime mover costs), illustrating the importance of considering the prime mover in future fuel selection.

The impact of operating profile, particularly the division between efficient fuel cells and gas turbine boost machinery is important, and is an area for further investigation. This may enable dual fuel arrangements, especially if multi-fuel capable high temperature fuel cells become available.

As with the OPV study, future fuels and machinery were seen to lead to some changes in overall ship layout "style". The concept of distributed generation, with fuel cells spread along the ship, was found to be attractive, addressing the layout issues caused by their increased volume. The higher fuel fraction required for alternative fuels may lead to ships with either reduced freeboard per unit displacement, or more spacious upper hull.

## 10. Acknowledgements

Development of ZEOLIT was carried out as part of the Preliminary Ship Design General Arrangements NICOP project and its successor NICOP, both funded by Ms. Kelly Cooper from the US Navy Office of Naval Re-search, and this support is gratefully acknowledged. The conclusions presented are the opinions of the authors.

## 11. References

[Advanced Propulsion Centre, 2020] Advanced Propulsion Centre UK, Fuel Cell Roadmap 2020, ISBN 978 1 78413 493 8

[Astley, Grasman, & Stroeve, 2020] Astley, W. E., Grasman, A. & Stroeve, D. B., “Exploring the Impact of Methanol as an Alternative, Cleaner Fuel for the Auxiliary and Support Vessels Within the RNLN”, Proc. INEC 2020, IMarEST, October 2020

[Bossel, 2005] Bossel, U, "Solid Oxide Fuel Cells for Transportation", Journal of KONES Internal Combustion Engines 2005, vol. 12, 3-4

[Brack, Birdsey & Walker, 2021] Brack, D., Birdsey, R. & Walker, W., “Greenhouse gas emissions from burning US-sourced woody biomass in the EU and UK”, Chatham House 2021.

[Corvus Blue Whale, 2022] Corvus Blue Whale page: https://corvusenergy.com/products/energy-storage-solutions/corvus-blue-whale/

[DNV, 2022] DNV, “Alternative Fuels for Naval Vessels”, white paper, 2022

[DNV-GL, 2019] DNV-GL, Comparison of Alternative Marine Fuels, Report No.: 2019-0567, Rev. 3, July 2019

[Duong et al. 2022] Duong, P.A., Ryu, B., Kim, C, Lee, J. & Kang, H., “Energy and Exergy Analysis of an Ammonia Fuel Cell Integrated System for Marine Vessels”, Energies 2022, 15, 3331

[Jensen, 2019] Jensen, M. F., "Blue World Technologies", Methanol Vehicles Exhibition, Chongqing, October 2019

[Krants, Søgaard & Smith, 2022] Krants, R., Søgaard, K. & Smith, T., “The scale of investment needed to decarbonize international shipping”, Global Maritime Forum, https://www.globalmaritimeforum.org/news/the-scale-of-investment-needed-to-decarbonize-international-shipping

[Kuseian & Hoffman, 2002] Kuseian, J & Hoffman, D, “Navy Shipboard Fuel Cell Program”, U.S. Maritime Administration Workshop on Maritime Energy and Clean Emissions, January 2002

[Kyocera, 2017] Kyocera: “KYOCERA Develops Industry’s First 3-Kilowatt Solid-Oxide Fuel Cell for Institutional Cogeneration”, July 6, 2017, https://global.kyocera.com/news/2017/0702_bnfo.html

[Mitsubishi Power, 2021] Mitsubishi Power Sustainable Energy Solutions, Solid Oxide Fuel Cell System, Mitsubishi Power Europe GmbH, 07.07.21

[Pawling, 2022a] Pawling, R. J., “The Zoom Years: UCL MSc Student Warship Designs Through the Pandemic”, RINA Warship 2022, 8th – 9th June 2022, Bristol, UK

[Pawling, 2022b] Pawling, R. J., “Examining The Impact Of Future Alternative Fuels On Naval Vessels”, RINA Warship 2022, 8th – 9th June 2022, Bristol, UK

[Pawling, Farrier & Bradbeer, 2018] Pawling, R.J., Farrier, L. & Bradbeer, N., “The Advanced Technology Corvette (Railgun): A Concept Exploration of Future Warships”, International Conference Warship 2018: Procurement of Future Surface Vessels, RINA, London, June 2018.

[Pawling, Farrier & Bucknall, 2018] Pawling, R.J., Farrier, L. & Bucknall, R.W.G., “The Advanced Technology Corvette - Railgun (ATK-R) Design Study - Future Weapons and Small Ship Power Systems”, Proc. International Naval Engineering Conference (INEC) 2018, Institute of Marine Engineering, Science and Technology (IMarEST), Glasgow, UK

[Pratt & Chan, 2017] Pratt, J. W. & Chan, S. H., “Maritime Fuel Cell Generator Project”, Sandia report SAND2017-5751, May 2017

[Rude et al., 2022] Rude, T., Durr, S., Preuster, P., Wolf, M. & Wasserscheid, P., “Benzyltoluene/perhydro benzyltoluene – pushing the performance limits of pure hydrocarbon liquid organic hydrogen carrier (LOHC) systems”, Sustainable Energy Fuels 2022, 6, 1541

[Sasaki et al., 2004] Sasaki, K., Watanabe, K., Shiosaki, K., Susuki, K. & Teraoka, Y., “Multi-Fuel Capability of Solid Oxide Fuel Cells”, Journal of Electroceramics volume 13, pages 669–675 (2004)

[Shintaro et al., 2020] Shintaro, I., Masahiro, U., Toshiyuki, S. & Toshiro, F., “Development of Ammonia Gas Turbine Co-Generation Technology”, IHI Engineering Review, Vol. 53, No. 1, 2020

[Tol & Linden, 2018] Tol, R. & Linden, Y., “Effect of Gas-to-Liquid (GTL) Fuels on Marine Diesel Engines Compared to F-76”, Proc. INEC 2018, IMarEST, October 2018

[Whyatt & Chick, 2012] Whyatt G.A. & Chick L.A.: “Electrical Generation for More-Electric Aircraft using Solid Oxide Fuel Cells”, PNNL-21382, US DoE, April 2012

Word count ~4750